Uncertainties in fertilizer-induced emissions of soil nitrogen oxide and the associated impacts on ground-level ozone and methane

- Cheng Gong^{1*}, Yan Wang², Hanqin Tian^{3,4}, Sian Kou-Giesbrecht⁵, Nicolas Vuichard⁶ and Sönke Zaehle¹
- ¹Max Planck Institute for Biogeochemistry, Jena, 07745, Germany
- 6 ²State Key Laboratory of Subtropical Silviculture, College of Environment and Resources, College of
- 7 Carbon Neutrality, Zhejiang A&F University, Hangzhou, 311300, China
- 8 ³Center for Earth System Science and Global Sustainability, Schiller Institute for Integrated Science
- 9 and Society, Boston College, Chestnut Hill, MA, USA
- ⁴Department of Earth and Environmental Sciences, Boston College, Chestnut Hill, MA, USA
- ⁵Simon Fraser University, Canada
- ⁶Laboratoire des Sciences du Climat et de l'Environnement, LSCE-IPSL (CEA-CNRS-UVSQ),
- 13 Université Paris-Saclay, Gif-sur-Yvette, France

14 15

16

17

18 19

20 21

22

23

2425

26

2728

29

30

31

32

1 2

Abstract

Natural and agricultural soils are important sources of nitrogen oxides (NO_x), accounting for about 10%-20% of the global NO_x emissions. The increased application of nitrogen (N) fertilizer in agriculture has strongly enhanced the N availability of soils in the last several decades, leading to higher soil NO_x emissions. However, the magnitude of the N fertilizer-induced soil NO_x emissions remains poorly constrained due to limited field observations, resulting in divergent estimates. Here we integrate the results from meta-analyses of field manipulation experiments, emission inventories, atmospheric chemistry modelling and terrestrial biosphere modelling to investigate these uncertainties and the associated impacts on ground-level ozone and methane. The estimated present-day global soil NO_x emissions induced by N fertilizer application vary substantially (0.84–2.2 Tg N yr⁻¹) among different approaches with different spatial patterns. Simulations with the 3-D global chemical transport model GEOS-Chem demonstrate that N fertilization enhances global surface ozone concentrations during summertime in agricultural hotspots, such as North America, western Europe and eastern and southern Asia by 0.1 to 3.3 ppbv (0.2%-7.0%). Our results show that such spreads in soil NO_x emissions also affect atmospheric methane concentrations, reducing the global mean by 6.7 (0.4%) ppby to 16.6 (0.9%) ppby as an indirect consequence of enhanced N fertilizer application. These results highlight the urgent need to improve the predictive understanding of soil NO_x emission responses to fertilizer N inputs and its representation in atmospheric chemistry modelling.

33

34

*Correspondence to: Cheng Gong (cgong@bgc-jena.mpg.de)

35 1. Introduction

36 37 strongly affect the atmospheric oxidation capacity and further influence air quality (Gong et al., 2020; Zhai et al., 2021; Goldberg et al., 2022; Zhao et al., 2023), radiative forcing (Erisman et al., 2011; Pinder 38 39 et al., 2012; Gong et al., 2024), as well as carbon (C) storage in terrestrial and marine ecosystems 40 (Fowler et al., 2013; Fleischer et al., 2019; Rubin et al., 2023). The major source of present-day 41 atmospheric NO_x is fossil fuel combustion (Martin et al., 2003; Hoesly et al., 2018), but several non-42 fossil-fuel sources, including emissions from soils, lightning and wildfire (Zhang et al., 2003), 43 contribute around 30% of the global total NO_x emissions (Delmas et al., 1997; Weng et al., 2020). 44 However, these non-fossil-fuel sources have been widely regarded as 'natural' sources, where the 45 perturbation by anthropogenic activities as well as the associated potentially significant effects on the 46 N cycle are often overlooked. Meanwhile, strict clean-air actions have been applied in many countries 47 in the past decades to sharply reduce the fossil-fuel sources of NO_x (Jiang et al., 2022). As a result, nonfossil sources of NO_x will be increasingly important for future clean air policies. 48 One of the most important non-fossil-fuel anthropogenic sources of NO_x is through agricultural 49 50 activities, which have been estimated to enhance soil NO_x emissions by around 5%-30% (Wang et al., 51 2022; Gong et al., 2024). To assess the soil NO_x emissions induced by N fertilizer application (hereafter, 52 SNO_x-Fer), the most straightforward and widely-used method is applying the emission factor (EF), 53 which indicates the proportion of N from fertilizer application emitted as NO_x. The Intergovernmental 54 Panel on Climate Change (IPCC) methodology recommended a constant EF value of 1.1% with an 55 uncertainty range of 0.06% to 2.18% (Hergoualc'h et al., 2019). Other studies recommend slightly 56 smaller uncertainty ranges (0.47% to 1.61%) based on different meta-analysis datasets (Stehfest and 57 Bouwman, 2006; Liu et al., 2017; Skiba et al., 2021; Wang et al., 2022). This large uncertainty range 58 results from the dependency of the response of soil NO_x emissions on intricate soil biogeochemical 59 processes, and it varies with crop types, soil texture, fertilizer types and application rate (Wang et al., 2022). To date, limited field experiments are available to constrain this uncertainty range. 60 Some studies have suggested using non-linear EF to take account of the observations that the EFs of 61 62 soil reactive nitrogen gases tend to increase with increasing fertilizer application (Shcherbak et al., 2014; 63 Jiang et al., 2017). Such an approach assumes that plants and soil microbes should have priority in 64 accessing soil available N for their metabolic activities, while the excessive inorganic N can be used by nitrifiers and denitrifiers and loses as the gas form. Such a non-linear EF approach is more ecologically 65 66 reasonable but there remain large uncertainties in assessing soil NO_x due to the limited available field 67 data. For example, Wang et al. (2024) examined the non-linear EF of soil NO_x based on a global meta-68 analysis and found a much lower EF (around 0-0.7%) than the IPCC-recommended linear EF (1.1%) 69 within the range of normal agricultural crop N fertilizer loading (around 0-600 kg N ha⁻¹ yr⁻¹).

Nitrogen oxides ($NO_x = NO + NO_2$), as one of the most important reactive atmospheric components,

70 In many of the atmospheric chemical transport models (CTMs), SNO_x-Fer is represented by the 71 agriculture sector of NO_x emission from an anthropogenic emission inventory (e.g. Emissions Database 72 for Global Atmospheric Research (EDGAR) or Community Emissions Data System (CEDS)), which in general apply the linear EF method to estimate the agricultural NO_x emissions (Hoesly et al., 2018; 73 74 Janssens-Maenhout et al., 2019; Nicholas Hutchings et al., 2023) with the caveats described above. 75 Furthermore, some advanced CTMs, e.g. the GEOS-Chem model, parametrize soil NO_x emissions as a 76 function of N availability as well as soil temperature and soil moisture (Steinkamp and Lawrence, 2011; 77 Hudman et al., 2012). The currently widely used soil NO_x scheme, known as the Berkeley-Dalhousie 78 Soil NO_x Parameterization (BDSNP), could dynamically simulate the spatiotemporal variations of soil 79 NO_x emissions, however, the responses of soil NO_x to N fertilizer application are not fully examined 80 (See the detailed parameterization in Sect. 2). Recently, another approach to modelling SNO_x-Fer has emerged with the development of global, 81 process-based terrestrial biosphere models (TBMs) with fully-coupled C and N cycles (Zaehle and 82 83 Friend, 2010; Tian et al., 2019). Driven by data of N inputs (synthetic N fertilizer, N manure application 84 and N deposition), CO₂ concentrations and climate, these TBMs could simulate the coupled cycles of 85 C and N in the terrestrial biosphere, mimic the competition on the available N between plants and 86 microbes and calculate the rates of nitrification and denitrification (Zaehle and Dalmonech, 2011), 87 which are the two microbial processes that determine the rates of soil NO_x emissions. Even though 88 TBMs provide a more ecologically-mechanistic description of the terrestrial N cycles, large 89 uncertainties remain among different TBMs due to the varying parameterization and modelling schemes 90 in biome N use strategies, mineralization of organic N, nitrification and denitrification processes (Kou-91 Giesbrecht et al., 2023), which lead to varied responses of soil NO_x to the increased N fertilizer inputs 92 (Gong et al., 2024).

In this study, we attempt to comprehensively quantify the uncertainties in current SNO_x-Fer estimates by integrating results from meta-analyses, emission inventories, as well as CTMs and TBMs. We use this understanding to assess the associated effects of SNO_x-Fer uncertainties on global O₃ and CH₄ concentrations. Section 2 will introduce the N synthetic fertilizer and manure input data and the approaches used to estimate SNO_x-Fer. Section 3 will introduce the CTM used in this study and the configuration of sensitivity experiments. Section 4 will first show the variations of SNO_x-Fer among different approaches as well as the seasonal dynamics, and then analyze the associated uncertainties in global O₃ and CH₄ simulations. Finally, the conclusion and discussions of this study will be given in Section 5.

102

103

104

93

94 95

96

97 98

99

100

101

2. Data and Methods

2.1. Linear and Non-linear EFs and the global fertilizer N dataset

We first implement the most traditional method with a constant EF value to estimate the effects of N fertilizer application on soil NO_x emissions, where the value of 1.1% (1.1% of N in the fertilizer will

be emitted as NO_x ; named EF_{linear} hereafter) based on the most up-to-date IPCC methodology is adopted

108 (Hergoualc'h et al., 2019). Furthermore, based on the latest meta-analysis dataset developed by Wang

et al. (2024), a non-linear EF method ($EF_{non-linear}$) to describe the variations of soil NO_x emissions with

different N fertilizer loadings is also applied:

$$EF_{non-linear} = (0.22 + 0.008 \times Fertilizer_N)$$
 (1)

- where the $EF_{non-linear}$ (%) is the non-linear EF and $Fertilizer_N$ is the loading of fertilizer N application
- 113 (kg N ha⁻¹). The detailed derivation of this formula is presented in Wang et al. (2024), which follows a
- comparable method as presented by Shcherbak et al. (2014).
- We used the dataset of History of anthropogenic Nitrogen inputs (HaNi) (Tian et al., 2022) for the
- 116 global rate of synthetic fertilizer and manure application, in order to estimate SNO_x-Fer with both the
- linear and non-linear EF methods. The HaNi dataset includes grid-level annual loadings of (1) NH₄+N
- synthetic fertilizer applied to cropland, (2) NO₃-N synthetic fertilizer applied to cropland, (3) NH₄+N
- synthetic fertilizer applied to pasture, (4) NO₃-N synthetic fertilizer applied to pasture, (5) manure
- 120 NH₄⁺-N application on cropland, (6) manure NO₃⁻-N application on pasture, (7) manure NH₄⁺-N
- deposition on pasture, and (8) manure NO_3 -N deposition on rangeland. We use a global map of land
- use class distribution (Hurtt et al., 2020) (Fig. S1) to convert the unit of N loading in HaNi from g N
- grid⁻¹ to kg N (ha pasture)⁻¹, kg N (ha rangeland)⁻¹ or kg N (ha cropland⁻¹). The annual N inputs from
- the HaNi dataset, which are summed by all N forms of synthetic fertilizer and manure, are evenly
- applied in the months of the growing season, while the rates of N inputs are set as zero during the non-
- growing season. We define the growing season as monthly-mean 2-metre temperature greater than 5
- degrees Celsius (based on the MERRA2 reanalyzed dataset, see below Sect. 3) and the grid-level
- monthly-mean leaf area index (LAI) larger than 0.5 (based on the MODIS remote sensing dataset post-
- 129 processed by Yuan et al. (2011) and updated for the use of GEOS-Chem,
- 130 http://geoschemdata.wustl.edu/ExtData/HEMCO/Yuan XLAI/v2021-06/). Finally, the rates of
- synthetic fertilizer and manure N inputs in units of kg N (ha pasture/rangeland/cropland)⁻¹ month⁻¹ are
- utilized to estimate global SNO_x-Fer with both the linear and non-linear EF approaches (Fig. S2).
- 133 2.2. The emissions inventory CEDS
- We use the CEDS (Hoesly et al., 2018) for assessing the fertilizer-induced soil NO_x emissions in the
- emission inventories. CEDS is one of the most state-of-the-art emission inventories that
- comprehensively assesses the sources of dominant air pollutants from the pre-industrial period to the
- present day, which has been used as the standard emission inventory to drive CMIP6 models. The
- agricultural NO_x emission in CEDS is fromEDGAR 4.3.1 (https://edgar.jrc.ec.europa.eu/), where the

- old IPCC methodology (Eggleston et al., 2006) is used with a constant EF value of 0.7% (0.7% of N in
- the fertilizer will be emitted as NO_x) (Janssens-Maenhout et al., 2019).
- 141 2.3. The BDSNP scheme
- The BDSNP scheme in CTMs was firstly developed by Yienger and Levy (1995), and then updated by
- Hudman et al. (2012). The emission of soil NO_x (S_{nox}) is described as:

144
$$S_{nox} = (A_{w.biome} + N_{avail} \times \bar{E}) \times f(T) \times g(\theta) \times P(l_{drv})$$
 (2)

- Where f(T), $g(\theta)$ and $P(l_{dry})$ indicate the effects of temperature, soil moisture and rain pulsing. $A_{w,biome}$
- is the wet biome-dependent emission (the baseline emission) from Steinkamp and Lawrence (2011).
- 147 N_{avail} is the soil available N mass in the top 10 cm (ng N m⁻²), which is calculated by:

148
$$N_{avail}(t) = N_{avail}(0)e^{-\frac{t}{\tau}} + Fertilizer_N \times \tau \times (1 - e^{-\frac{t}{\tau}})$$
 (3)

- Where the initial soil available N mass $N_{avail}(0)$ is prescribed. Fertilizer N is the rate of fertilizer N
- application, which is set to zero outside the growing season. τ indicates the decay rate and is chosen as
- 4 months based on the measurements within the top 10 cm of soil (Matson et al., 1998; Cheng et al.,
- 2004; Russell et al., 2011). However, it should be noted that the magnitude of global SNO_x-Fer (i.e. the
- 153 $N_{avail} \times \bar{E}$) is scaled by the factor \bar{E} in Eq. (2) to meet 1.8 Tg N yr⁻¹ before the canopy reduction, which
- is the value obtained in a previous meta-analysis study based on the fertilizer N input dataset in the
- 2000s (Stehfest and Bouwman, 2006). As a result, the default BDSNP scheme in GEOS-Chem actually
- fails to capture the year-to-year variations of soil NO_x emissions with the changing soil N availability.
- However, as the BDSNP scheme is still widely used by the community of atmospheric chemistry
- modelling (e.g. Lu et al., 2021; Wang et al., 2022; Huber et al., 2023), here we add another sensitivity
- experiment by scaling the N_{avail} in Eq.3 following the interannual variations of the HaNi fertilizer
- 160 loadings:

$$161 N_{avail}(i,j,yr) = N_{avail}(i,j,2000) * \frac{Fertilizer_{HaNi}(i,j,yr)}{Fertilizer_{HaNi}(i,j,2000)}$$

$$(4)$$

- Where $Fertilizer_{HaNi}(i, j, yr)$ represents the total N fertilizer loadings in the HaNi dataset at the grid
- of i latitude and j longitude in the yr year. With this modification, we could further examine how SNO_x-
- Fer responds to the N fertilizer enhancement in the GEOS-Chem BDSNP scheme.
- 165 2.4. The TBM ensemble
- Simulated soil NO_x emissions were provided by three TBMs (CLASSIC, OCN and ORCHIDEE) with
- fully-coupled C and N cycles included in the global nitrogen/N₂O model inter-comparison project phase
- 2 (NMIP2) (Tian et al., 2024). For each TBM model, anthropogenic fertilizer applications are estimated
- by the HaNi dataset (Tian et al., 2022), where the fertilizer types (NH₄⁺ and NO₃⁻; synthetic fertilizer

and manure) are explicitly distinguished in the model. The SNO_x-Fer can be isolated by summing up the differences between sensitivity experiments SH1 and SH2 (the synthetic fertilizer contribution) and the differences between sensitivity experiments SH1 and SH3 (the manure contribution) (Table S1). It should be noted that the CLASSIC model did not isolate synthetic fertilizer and manure and thus only conducted one sensitivity experiment. The model ensemble mean is utilized to smooth the large discrepancies among different TBMs (Fig. S3) due to the varied terrestrial N-cycle representations, in particular, the varied nitrification and denitrification rates.

3. The GEOS-Chem model and sensitivity experiment configuration

The GEOS-Chem model is a frequently used state-of-the-art CTM with fully coupled NOx–Ox–hydrocarbon–aerosol chemistry mechanism (Bey et al., 2001; Park et al., 2004). Here we applied version 12.0.0 to run the global simulation with a horizontal resolution of 2° latitude × 2.5° longitude. The simulations are driven by the Version two of modern era retrospective-analysis for research and application (MERRA2) reanalyzed meteorological dataset. The photolysis rates were computed by the Fast-JX scheme (Park et al., 2004). The atmospheric gas-phase chemistry is independently developed referring to the kinetics and products based on JPL recommendations (Bates et al., 2024) and solved by the Kinetic Pre-Processor (KPP) (Henze et al., 2007). Aerosol thermodynamic equilibrium is calculated by the ISORROPIA II package (Fountoukis and Nenes, 2007). In particular, the default soil NO_x emissions are simulated by the BDSNP scheme as introduced above.

In order to examine the uncertainties in SNO_x-Fer and the associated effects on global surface O₃ concentrations, we first ran a reference simulation in 2019 (named Zero) with zero SNO_x-Fer to exclude the influence of fertilizer application on soil NO_x. Then eleven different experiments were performed by representing SNO_x-Fer with CEDS agricultural NO_x emissions (named CEDS), the default GEOS-Chem BDSNP scheme (Eqs. 2-3, named BDSNP_coarse), the BDSNP scaled by the interannually varied HaNi N fertilizer loadings (Eq. 4, named BDSNP_coarse_scaled), the default GEOS-Chem BDSNP but with fine resolution of 0.5°× 0.625° (named BDSNP_fine), the TBM-simulated SNO_x-Fer of each model as well as the ensemble mean (named NMIP2-OCN, NMIP2-CLASSIC, NMIP2-ORCHIDEE and NMIP2, respectively), the linear EF (EF=1.1%) method (named Linear) and the nonlinear EF (Eq. 1) method (named Nonlinear), respectively. In particular, the BDSNP_fine is simulated offline, i.e., the atmospheric chemical and transport processes are not accounted due to the inconsistency of resolutions with the GEOS-Chem runs. All of the sensitivity experiments are driven by the meteorological field in 2019 with 6-month spin up, where the anthropogenic emissions of all other tracers also keep at the 2019 level following the CEDS inventory. Table 1 summarizes the eleven sensitivity experiments in GEOS-Chem.

In order to further examine the seasonality of SNO_x-Fer and the associated impacts on ground-level O₃ in agricultural hotspot regions, we investigate how different SNO_x-Fer approaches distribute the annual fertilizer seasonally (Table 1). The HaNi dataset, as well as the equivalently up-to-date fertilizer dataset (Adalibieke et al., 2023), only provide annual fertilizer application rates given the lack of specific information to distribute N fertilization seasonally. The CEDS, BDSNP and NMIP2 model approaches have their own specific monthly distribution, while the monthly distribution of fertilizer application in the linear and nonlinear EF is arbitrarily assumed to be even during the growing season. Here, we added two additional GEOS-Chem sensitivity experiments for the linear and non-linear approach, named Linear_7525 and Nonlinear_7525, which apply the seasonal pattern of the BDSNP scheme (Hudman et al., 2012), assuming that 75% of the annual fertilizer is applied in the first month of the growing season and the remaining 25% evenly applied in the rest of the growing months.

Table 1. Summary of the sensitivity experiments in GEOS-Chem and the methods used by different SNO_x -Fer estimating approaches to distribute the annual N fertilizer into monthly.

SNO _x -Fer estimating approch	Experimental name in this study	Emissions of SNO _x -Fer	Fertilizer monthly distribution	
None	Zero	Zero	None	
	Linear	Linear EF	Evenly distributed during the growing season	
Emission Factor (EF)	Nonlinear	Nonlinear EF		
	Linear_7525	Linear EF	75% of the annual fertilizer is applied in the first month of	
	Nonlinear_7525	Nonlinear EF	growing season, while the rest 25% is evenly distributed in the rest growing months	
Emission inventory	CEDS	CEDS agricultural NO _x sector	Not clear	
BDSNP	BDSNP_coarse	GEOS-Chem default BDSNP with resolution of 2°×2.5°	75% of the annual fertilizer is applied in	
	BDSNP_coarse_scaled	BDSNP scaled with the interannual variations of HaNi fertilizer loadings with resolution 2°×2.5°	the first month of growing season, while the rest 25% is evenly distributed in the rest	
	BDSNP_fine (offline)	GEOS-Chem default BDSNP with resolution of $0.5^{\circ} \times 0.625^{\circ}$	growing months	

Terrestrial biosphere models (TBMs)	NMIP2-OCN	OCN simulated SNO _x -Fer	Distributed the annual N fertilizer loadings into four equal doses in the first half of the growing season
	NMIP2-CLASSIC	CLASSIC simulated SNO _x -Fer	Evenly distributed throughout the year in the tropics (between 30S and 30N); Evenly distributed from spring equinox to fall equinox between 30N (30S) and 90N (90S)
	NMIP2-ORCHIDEE	ORCHIDEE simulated SNO _x -Fer	Half of the annual N fertilizer applied on the first day of the growing season; The remaining half applied on the 30th day since the beginning of the growing season
	NMIP2	TBMs ensemble mean	

Because the default GEOS-Chem simulations used above do not account for interactive CH₄ chemistry, we further conducted ten more sensitivity experiments with the special 'CH₄ run' in GEOS-Chem (East et al., 2024; Fu et al., 2024) to assess variations in the atmospheric CH₄ concentrations induced by the uncertain SNO_x-Fer. The special CH₄ run takes CH₄ as the sole atmospheric transport tracer with various prescribed CH₄ sources (summarized in Table S2), while the CH₄ sinks include the tropospheric reactions with hydroxyl radical (OH) and chlorine, stratospheric loss and soil uptake. The global monthly mean OH concentrations archived from the ten sensitivity experiments (Table 1, except for the BDSNP_fine) are applied in the CH₄ simulation to assess the SNO_x-Fer effect on CH₄ lifetime through perturbing atmospheric oxidation capacity. As a result, there are ten more associated sensitivity experiments with the CH₄ run that correspond to the default GEOS-Chem simulations in Table 1 (except for the BDSNP_fine experiment). Each CH₄ simulation ran for 15 years by repeating the meteorological forcings in 2019 to reach a semi-equilibrium with the prescribed emissions and OH concentrations. The last year of the simulation was utilized to analyze the influences of soil NO_x on CH₄ induced by N fertilizer application. The simulated global surface CH₄ concentrations driven by varied OH levels from different sensitivity experiments are shown in Fig. S5.

4. Results

4.1 Varied SNO_x-Fer among different approaches

Figure 1 shows the historical time series of global SNO_x-Fer over 1950-2019 estimated by different approaches, mainly driven by the substantial increases in global N fertilizer application. Almost all approaches except BDSNP showed enhancements in soil NO_x emissions but with largely varied magnitudes from 0.6 to 2.1 Tg yr⁻¹ over 1950-2019. The default BDSNP scheme in GEOS-Chem, which scales soil NO_x emissions with time-variant temperature and soil moisture, but assumes constant N availability (see Methods), estimates relatively stable soil NO_x emissions over 1980-2019. The annually-varied BDSNP scheme scaled by the HaNi N input dataset shows an increase in SNO_x-Fer from 0.8 Tg N yr⁻¹ in 1980 to 1.5 Tg N yr⁻¹ in 2019, while the sharpest increase in the soil NO_x emission is simulated by the TBM ensemble, mainly induced by the high estimates of the CLASSIC and ORCHIDEE models (Fig. S3). Soil NO_x estimated by the non-linear EF approach shows a substantially weaker response to fertilizer inputs relative to other estimating approaches.

Fertilizer-induced soil NO_x emissions

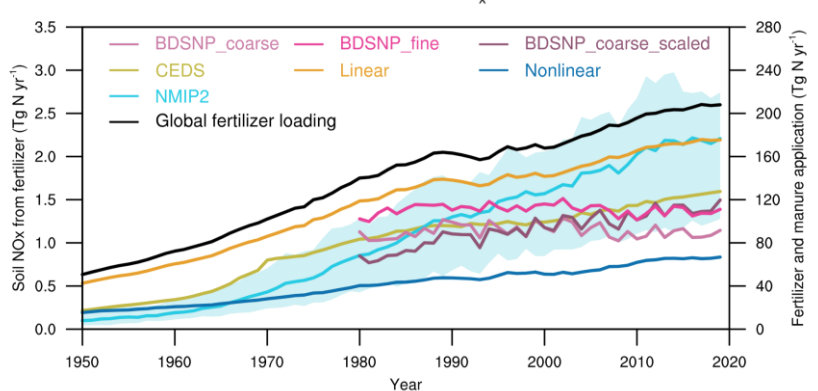


Figure 1. Global estimates of N fertilizer-induced soil NO_x emissions by different approaches. The black line (right Y axis) indicates global annual-mean N synthetic fertilizer and manure inputs over 1950-2019 assessed from the HaNi dataset. The remaining lines (left Y axis) indicate the N fertilizer-induced soil NO_x emissions over 1950-2019 estimated by different approaches, including the emission inventory (CEDS), linear and non-linear EF, the widely-used CTM parameterization with coarse resolution (2°×2.5°, BDSNP_coarse), fine resolution (0.5°×0.625°, BDSNP_fine) and interannually varied N availability (BNDSP_coarse_scaled), and the TBM ensembles (NMIP2). The light cyan shadows indicate the spread across three different TBMs in NMIP2.

Figure 3 shows the global spatial patterns of SNO_x-Fer among different approaches. Each approach shows consistent spatial patterns aligned with the distribution of N synthetic fertilizer and manure inputs (Fig. 2), where eastern U.S., western Europe, eastern and southern Asia are the hotspots with high soil NO_x emissions. Notably, even though the TBM ensemble (NMIP2) and the Linear EF approach estimate similar global total SNO_x-Fer, the spatial distributions of both estimates vary strongly. The SNO_x-Fer

estimates from the NMIP2 ensemble are higher in agricultural hotspots (Table 2), but lower in regions with less synthetic fertilizer application, e.g. in parts of the Africa and South America (Figs. 3d and 3e), relative to the Linear EF approach. It is because plants and microbes have high priority to assess additional N in N-limited regions, which leads less N loss as the gas forms. However, in N-saturated regions, the applied N fertilizer is excessive for the living biomes, yielding a higher sensitivity of soil NO_x emissions to N fertilizer application (Du and De Vries, 2025). Such N dynamics have been included in the C-N fully-coupled TBMs, but are not represented by the linear EF approach.

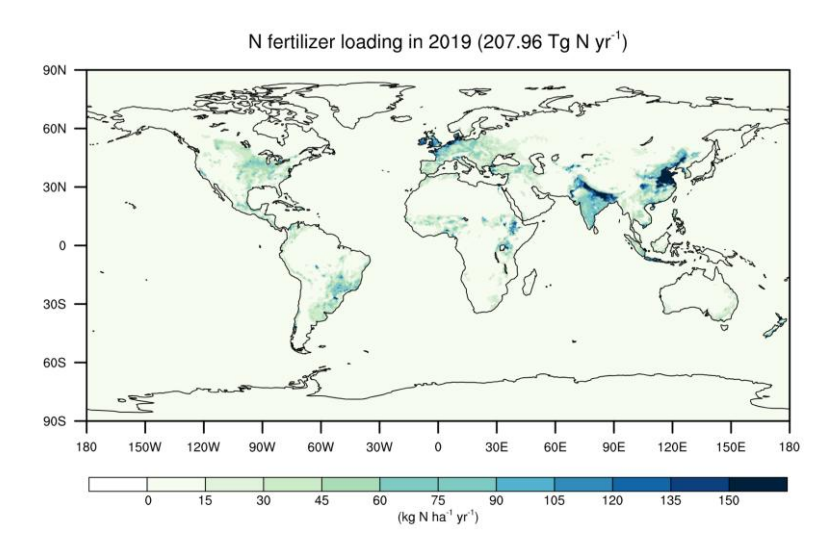
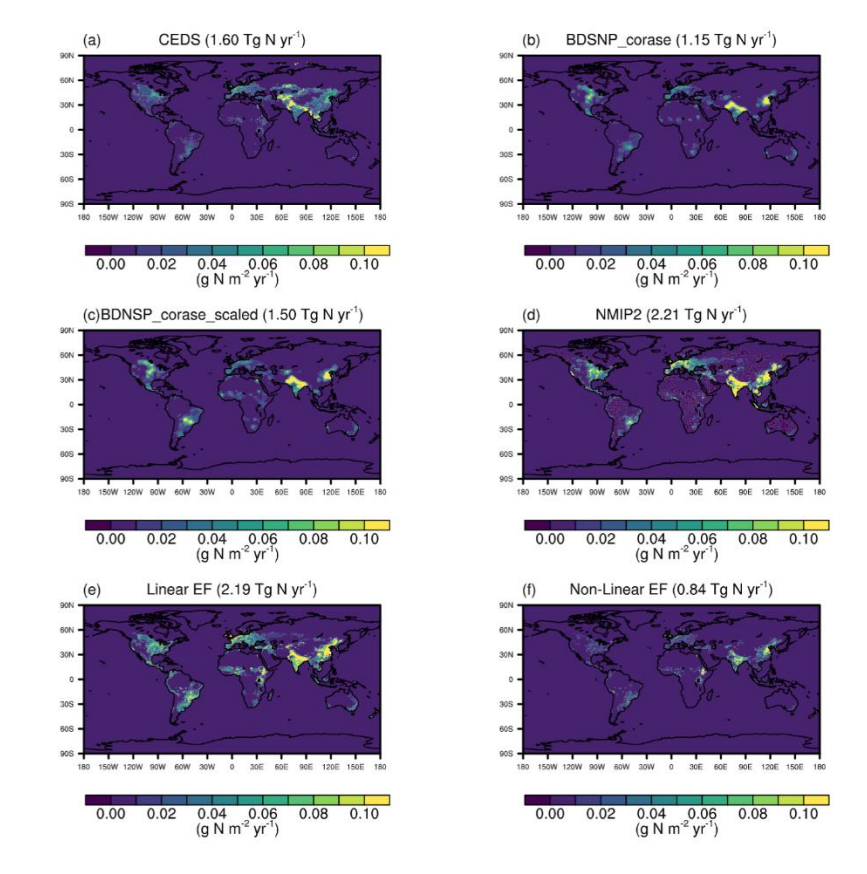


Figure 2. The global spatial patterns of N synthetic fertilizer and manure application in 2019 from the HaNi dataset.





276

279

280

281

282

Figure 3. The N-fertilization-induced soil NO_x emissions estimated by different approaches in 2019.

(a) - (f) The soil NO_x emissions induced by N fertilizer estimated by the CEDS agricultural sector, the default BDSNP scheme in GEOS-Chem with coarse resolution (2°×2.5°), the coarse-resolution BDSNP scheme in GEOS-Chem by interannually scaling the N availability using the HaNi dataset, the NMIP2 ensemble, the linear EF and non-linear EF, respectively. The global total budget of each estimate is given in the subtitles.

283

284

285286

Table 2. The annual soil NO_x emissions (Gg N yr⁻¹) induced by N fertilizer in 2019 in the eastern U.S., western Europe, eastern Asia, southern Asia and the global estimates by different approaches. The ranges in NMIP2 indicate the highest and lowest values among three TBMs (CLASSIC,

ORCHIDEE and OCN)

287

Eastern U.S. Western Europe Eastern Asia Southern Asia (35-45N, 75-(35-60N, 10W-(20-50N, 100-(10-30N, 70-Globe 90W) 20E) 125E) 85E) 99.1 190.0 **CEDS** 20.9 104.8 1600 BDSNP_corase 76.3 15.8 157.0 134.2 1150

BDSNP_corase_scaled	17.6	69.8	174.8	201.7	1500
NMIP2	57.0 [15.1, 100.9]	206.3 [67.4, 267.3]	417.5 [261.0, 598.1]	382.4 [78.4, 776.3]	2210 [1280, 2740]
Linear EF	54.3	181.0	376.4	214.7	2190
Non-Linear EF	15.6	60.8	136.5	141.8	840

289

290

291

292

293

294

295

296

297

298

299

300

301

302

303

304

305

306307

308

309

310311

312

313

314

315

316

4.2 The seasonal cycle of SNO_x-Fer and the associated impact on O₃ concentrations

Figure 4 shows the seasonality of SNO_x-Fer in four agricultural hotspot regions among different SNO_x-Fer estimating methods. In the temperate regions like Eastern U.S., Western Europe and Eastern Asia, the TBM ensemble NMIP2 shows very strong seasonal variations, which peaks during May to July in Eastern U.S., April to June in Western Europe and May to August in Eastern Asia, respectively. The seasonality of the linear and nonlinear EF methods is strongly dependent on the assumption of fertilizer application time (Table 1), where the monthly SNO_x-Fer emissions are at similar levels during the growing season for the Linear and Nonlinear experiments, but peak in a pronounced manner in the northern-hemispheric springtime (around February to April) in the Linear_7525 and Nonlinear_7525 cases. Although the BDSNP applies the same assumption of fertilizer application time as Linear 7525 and Nonlinear 7525, the SNO_x-Fer in BDSNP peaks much later (September to October in Eastern U.S., June to August in Western Europe and May to June in Eastern Asia). This arises because the EF methods estimate SNO_x-Fer instantaneously in response to the fertilizer application, but the BDSNP scheme cumulates N fertilizer with a 4-month time window (Eq. 3). It is also very important the BDSNP includes the regulation of soil temperature and moisture on SNO_x-Fer, both of which also have strong seasonality, but the EF methods do not. Furthermore, in the tropical regions of southern Asia, the NMIP2, Linear_7525 and Nonlinear_7525 experiments estimate the peak SNO_x-Fer in the beginning of the year, while the SNO_x-Fer of BDSNP reaches its highest in May due to the N cumulation assumption (Fig. 4d). The remaining methods, including the emissions inventory CEDS, the Linear and Nonlinear EF method, show very weak seasonality of SNO_x-Fer in Southern Asia.

The seasonality of ground-level monthly MDA8 O₃ changes in response to the SNO_x-Fer in general aligns with the monthly variations of SNO_x-Fer among different estimating approaches (Fig. 5). The strongest enhancement of regional MDA8 O₃ occurs during the northern-hemispheric summertime (June-August) for most of the estimating approaches in three temperate regions, when the absolute O₃ concentrations also reaches their highest. However, it should be noted that spring-peak SNO_x-Fer in the Linear_7525 and the Nonlinear_7525 cases does not lead to high O₃ enhancement in both western Europe and eastern Asia (Figs. 5b and 5c). The weak sensitivity of O₃ to NO_x during springtime is likely the result of the seasonal variations in other emissions (e.g. biogenic volatile organic compounds

(BVOCs)), which alter the chemical sensitivity regime. The responses of O₃ to SNO_x-Fer could also depend on the region (e.g. O₃ enhancement also peaks during spring in Linear_7525 in Eastern U.S., Fig. 5a), spatial simulation resolution or different modelling chemical mechanisms. The O₃ enhancement in southern Asia is generally similar during northern-hemispheric spring and summer time for all of the SNO_x-Fer estimating approaches (Fig. 5d), except for the BDSNP scheme, which simulates significantly higher O₃ enhancement during May to July relative to February to April.

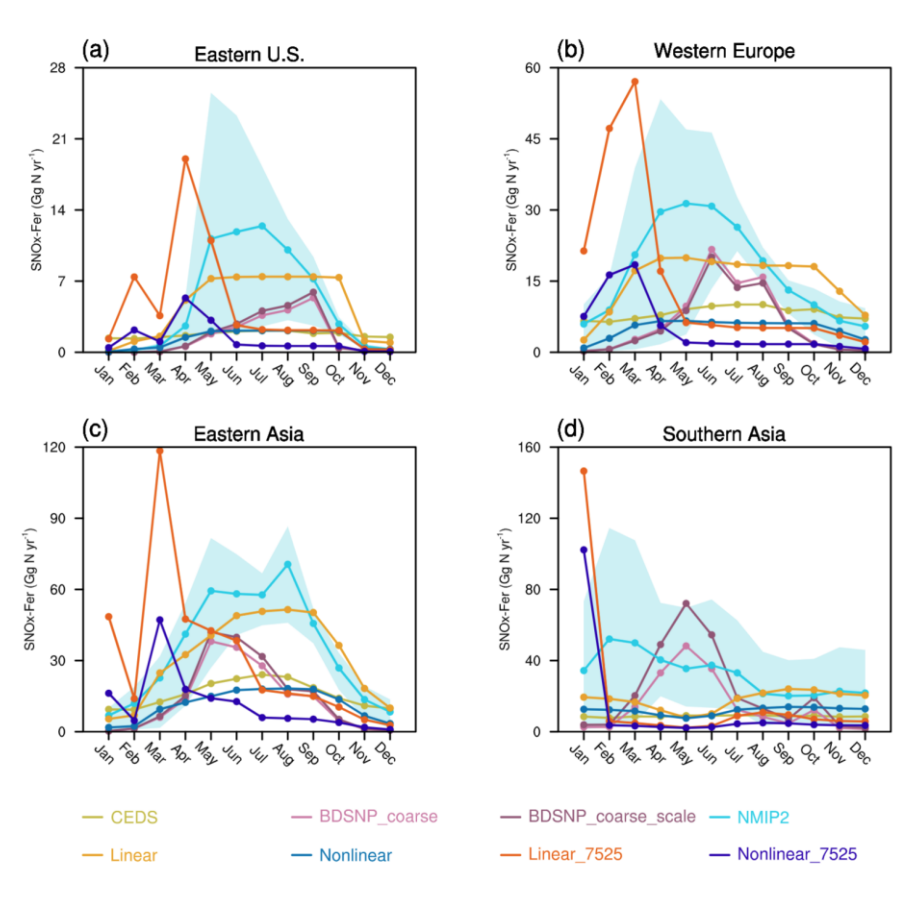


Figure 4. The monthly regional SNO_x -Fer (Gg N yr⁻¹) in (a) eastern U.S., (b) western Europe, (c) eastern Asia and (d) southern Asia with different SNO_x -Fer estimating approaches. The cyan-blue shades indicate the spread among three different TBM models (CLASSIC, OCN and ORCHIDEE) in the NMIP2 ensemble.

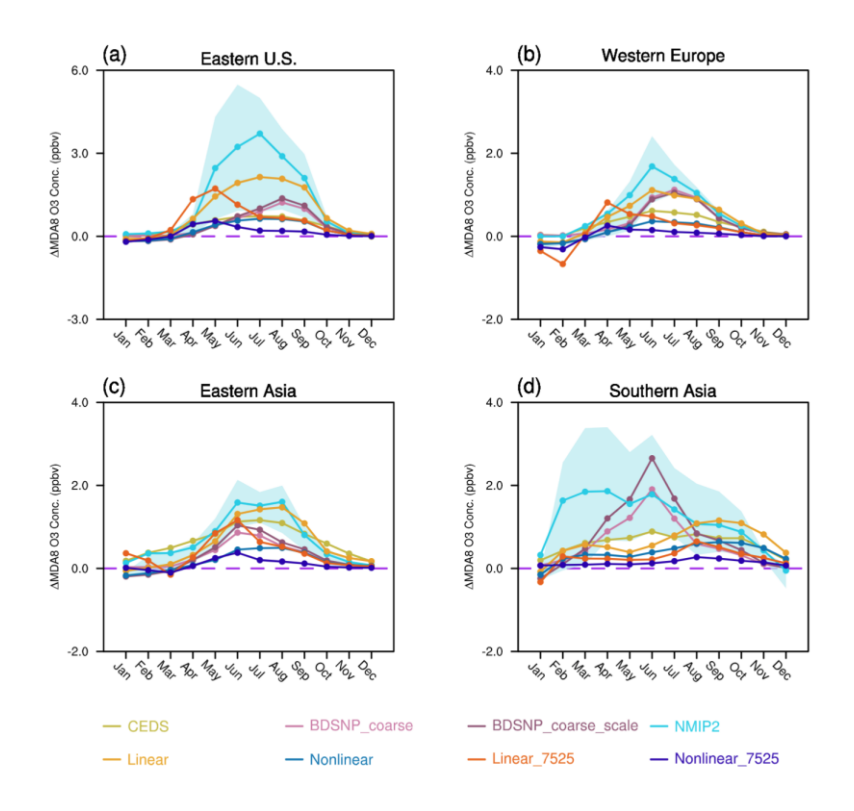


Figure 5. Regionally-averaged monthly MDA8 O_3 changes (ppbv) induced by SNO_x -Fer in (a) eastern U.S., (b) western Europe, (c) eastern Asia and (d) southern Asia with different SNO_x -Fer estimating approaches. The cyan-blue shades indicate the spread among three different TBM models (CLASSIC, OCN and ORCHIDEE) in the NMIP2 ensemble.

4.3 Impacts of SNO_x-Fer on surface O₃ concentrations

We next examine how the different SNO_x-Fer estimates influence the surface O₃ concentrations globally. Since soil NO_x emissions typically peak during the summer period (Fig. 4), when O₃ pollution tends to be most severe, we focus our analysis on the surface maximum daily 8-h averaged (MDA8) O₃ concentrations averaged over the northern hemisphere summer (June, July and August) based on the sensitivity experiments in Table 1. Figure 6 shows that the N fertilizer application enhanced the globally-averaged surface summertime O₃ MDA8 concentrations by 0.04-0.30 ppbv in 2019. In agricultural regions, the enhancement of O₃ concentrations due to SNO_x-Fer reaches 0.1-3.3 ppbv (0.2%-7.0%). Figure 6 also highlights important differences in the spatial effect of NO_x on O₃, consistent with the regional effects on SNO_x-Fer (Table 2), that the NMIP2 estimate of SNO_x-Fer shows stronger contributions to the O₃ concentrations than the linear EF approach in agricultural regions. The non-linear EF method leads to the lowest O₃ enhancement, although both non-linear EF and TBMs estimate increasing soil NO_x emissions with soil N availability.

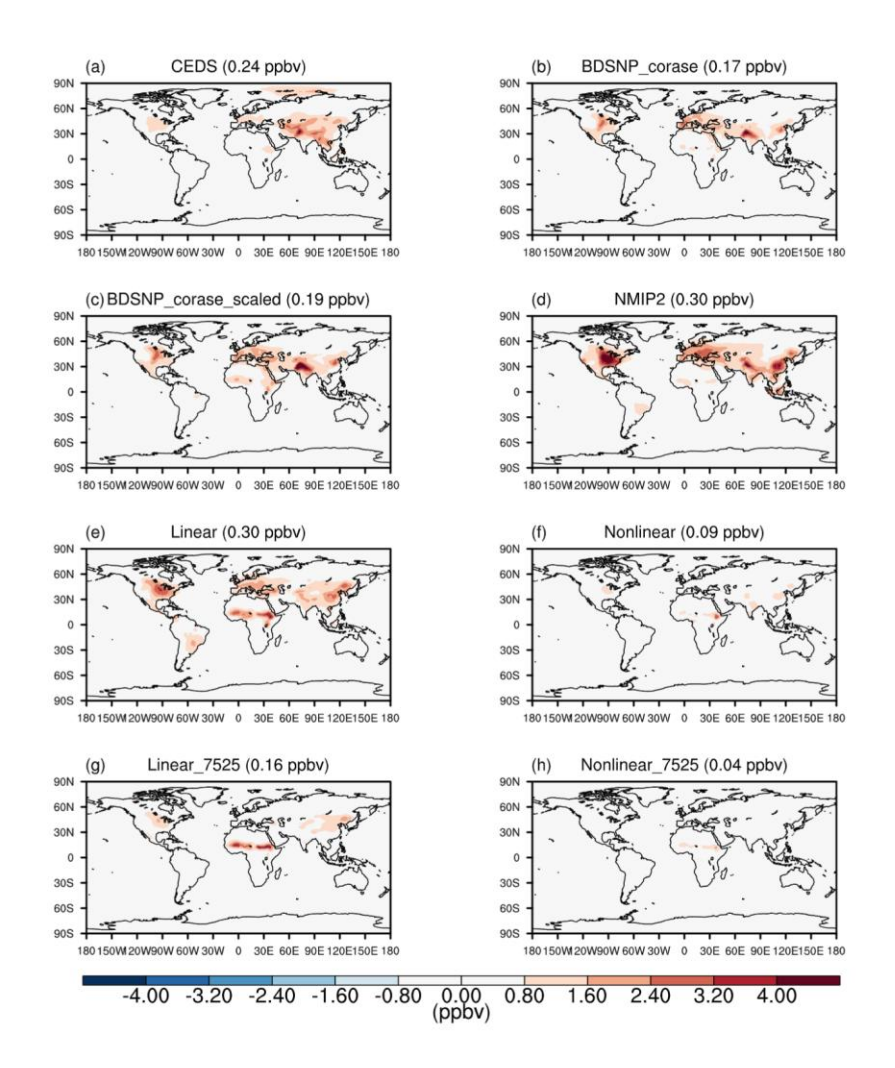


Figure 6. Global simulated changes in surface MDA8 O₃ concentrations induced by different estimating approaches of SNO_x-Fer averaged over June, July and August in 2019. The differences are calculated between corresponding sensitivity experiments in Table 1 and the Zero experiment. The numbers in each subtitle are changes in the globally averaged summertime MDA8 O₃ concentrations induced by SNO_x-Fer.

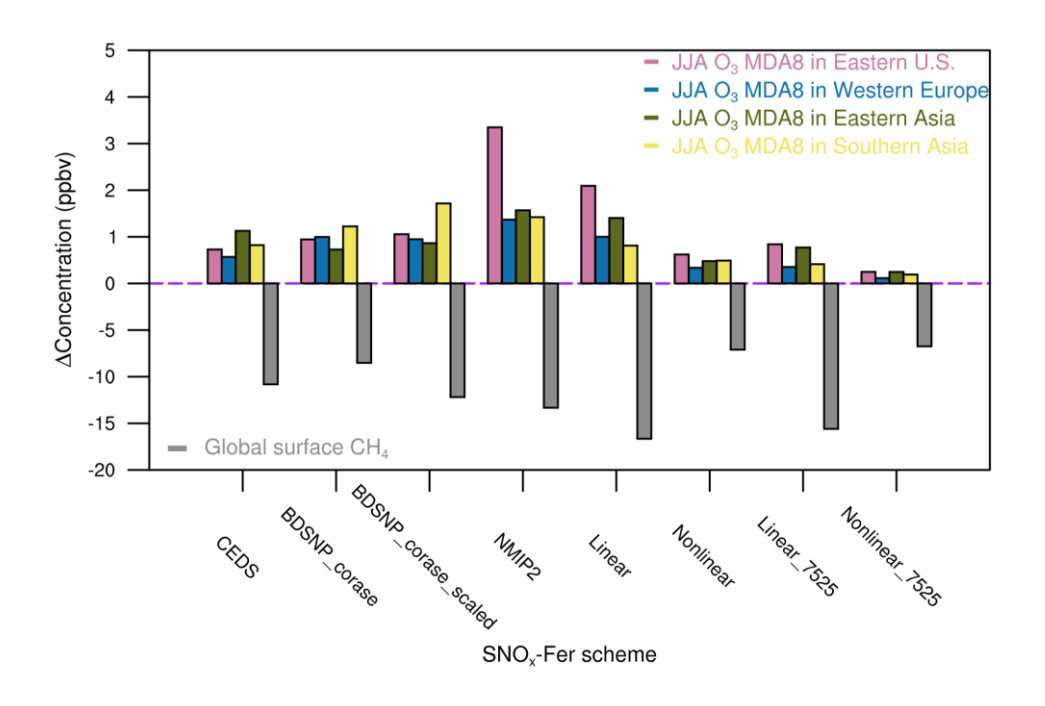


Figure 7. Changes in summertime averaged surface MDA8 O₃ concentrations (positive Y axis) and global surface CH₄ concentrations (negative Y axis) induced by SNO_x-Fer uncertainties. The regional MDA8 O₃ concentrations are averaged over eastern U.S. (35-45N, 75-90W), western Europe (35-60N, 10W-20E), eastern Asia (20-50N, 100-125E) and southern Asia (10-30N, 70-85E).

4.4 The impacts of SNO_x-Fer uncertainties on global CH₄ estimates

Figure 7 shows that N fertilizer-induced soil NO_x led to the reduction of globally averaged CH₄ concentrations ranging from 6.7 ppbv (0.4%) to 16.6 ppbv (0.9%) in 2019 by increasing atmospheric OH concentrations (Fig. S5), spatially aligned with the distributions of SNO_x-Fer among different estimating approaches (Fig. 3). Because CH₄ has a significantly longer atmospheric lifetime than either OH or NO_x, the spatial differences in the impacts of SNO_x-Fer on CH₄ concentrations are insignificant (Fig. S4). As a result, we only focus on the globally averaged changes in CH₄ concentrations. The magnitude of this estimate is consistent with the recent estimate of around 17.4 ppbv by Gong et al. (2024), which relies on the same NMIP2 dataset and a simpler CH₄ box model to calculate the impacts of NO_x emissions on the atmospheric lifetime of CH₄. This result highlights an important but indirect role of SNO_x-Fer on atmospheric CH₄ concentrations, which is an often-overlooked aspect for the global CH₄ budget. However, the uncertainty range in our estimates clearly suggests the need to further improve our understanding of soil N biogeochemical processes to better predict global OH reactivity and to better constrain global CH₄ budget.

5. Discussions

In this study, we integrated knowledge from meta-analyses (Hergoualc'h et al., 2019; Wang et al., 2024), the emission inventory, parameterizations in CTMs and the TBM ensembles to better quantify the uncertainties in N fertilizer-induced soil NO_x emissions and the associated impacts on global O_3 and CH_4 concentrations. Our results showed a large variation in the global soil NO_x emissions associated with N fertilizer, ranging from 0.84 Tg N yr $^{-1}$ to 2.2 Tg N yr $^{-1}$ in 2019. This range of responses leads to an enhancement in summertime surface MDA8 O_3 concentrations of 0.1 ppbv to 3.3 ppbv (0.2%-7.0%) in agricultural hotspot regions. The O_3 enhancement is highest in eastern U.S., while it is not only determined by the SNO_x-Fer emissions, but also the diverging sensitivities of O_3 to NO_x depending on different chemical regimes in GEOS-Chem (Fig. S6). The varied SNO_x-Fer estimates also lead to a reduction in global CH_4 concentrations of 6.7 ppbv (0.4%) to 16.6 ppbv (0.9%). These changes highlight a significant role of agricultural N use and soil N biogeochemical processes in affecting regional O_3 concentrations as well as controlling global greenhouse gases. In particular, with the worldwide reduction in fossil-fuel NO_x emissions associated with clean-air actions (Jiang et al., 2022), control of agricultural soil NO_x emissions becomes increasingly important to improve air quality and alleviate the associated public health risks.

However, challenges remain in the accurate assessment of N fertilizer-induced soil NO_x emissions. On the one hand, the overall uncertainties of SNO_x-Fer may still be underestimated. The EF-approach with fixed EF fails to adequately reflect the complexity in soil biogeochemical processes, which is reflected by the large ranges of EFs from 0.06% to 2.18% in a recent meta-analysis (Hergoualc'h et al., 2019). While the non-linear EF method represents an advance over the linear EF approach, as the effects of soil N saturation levels on soil N gas emissions are considered and therefore the approach yields relatively good performance in predicting soil N₂O or NH₃ emissions compared to observations (Shcherbak et al., 2014; Jiang et al., 2017), the limited availability of observations to constrain these responses and their limited spatiotemporal representativeness reduce the reliability of this approach. Most of the experimental data in Wang et al. (2024) are collected over China in the past ten years and thus may not be representative of other agricultural regions. Furthermore, 22 out of 55 data points are from vegetable cropping systems and orchard fields, where frequent irrigation may enhance soil moisture and thus inhibit the production of NO_x via nitrification. Last but not least, other factors, such as soil texture, pH, soil organic carbon and fertilizer types, may also affect the response of soil NO_x emissions to the loading of N fertilizer application, which are omitted by either the linear EF or nonlinear EF approach. As a result, more representative crop experiments with a gradient series of N addition are necessary to better constrain the soil NO_x response to N fertilizer application.

For the modelling of SNO_x-Fer, on the one hand, recent developments of the parameterization of BDSNP in CTMs focused more on the soil NO_x responses to changing temperature or soil moisture (e.g. Wang et al., 2021; Huber et al., 2023), while the accuracy of the soil N availability has been less

investigated. Even with the scaled N fertilizer loadings to interannually vary the N availability, BDSNP still showed a weaker increasing trend of SNO_x-Fer in response to the N fertilizer enhancement relative to the empirical EF methods and the TBM simulations of NMIP2 in the past decades (Fig. 1). Nevertheless, it should be noted that the BDSNP scheme is also sensitive to the spatial resolution, where the coarse resolution may miss small-scale hotspots and thus underestimate the global SNO_x-Fer, as the BDSNP_fine experiment shows in Fig. 1. On the other hand, terrestrial N availability is a key concept in the development of TBMs, as the process-based TBMs need a detailed description of the N cycle to understand nutrient limitation levels and associated C-N coupling. Nevertheless, the soil NO_x emissions have been overlooked by the ecological modelling community because the low emissions may not be important for the terrestrial N cycle, resulting in a limited number of TBMs that include soil NO_x emissions as well as large inter-model variations (Fig. S3). To further reduce the uncertainties in soil NO_x emission estimates, the advantages of TBMs on representing soil N availability can be introduced into CTMs to better examine the effects of agricultural activities on atmospheric chemistry, but at the same time, the terrestrial N cycle needs to be further developed in TBMs to reduce inter-model variations and to better predict soil emissions of reactive N gases (not only NO_x but also N₂O and NH₃). The seasonality of SNO_x-Fer and the associated impacts on surface O₃ concentrations are also important but poorly constrained. The most difficult challenge is to precisely estimate the monthly (or even daily) N fertilizer loadings on the global scale. Because the N fertilizer data underlying the gridded products is derived from the annual statistics by the Food and Agricultural Organization (FAO) (https://www.fao.org/faostat/en/#data), the HaNi dataset applied in this study, as well as the equivalently up-to-date fertilizer dataset (Adalibieke et al., 2023), only provides gridded, annual fertilizer application rates. In the EF approaches, the growing season is determined only by temperature and greenness in this study, which could result in a mismatch with the real crop or pasture calendar, especially ignoring the multiple-harvest crops per year. A refined calendar could further improve the prediction of SNO_x-Fer seasonality. Furthermore, the NO_x-VOCs-O₃ chemical sensitivity regimes could be determined not only by soil NO_x emissions, but also by other anthropogenic and biogenic emissions of NO_x and VOCs, as well as the climate seasonal variations. Therefore, the seasonal cycles of the enhancement of O₃ concentrations may not strictly follow the variations in SNO_x-Fer, as our Linear 75 sensitivity experiment implies in Western Europe and Eastern Asia (Figs. 5b and 5c). The impacts of the changes in short-lived air pollutants on the global CH₄ budget have attracted increasing attention in recent years (Peng et al., 2022; Zhao et al., 2025), where NO_x is one of the most important drivers. However, it should be noted that the sensitivity of CH₄ lifetime to NO_x emissions

415

416

417

418419

420

421

422

423

424

425

426

427

428 429

430

431

432

433

434

435

436

437438

439 440

441

442

443

444

445

446

447

448 449

450

important drivers. However, it should be noted that the sensitivity of CH_4 lifetime to NO_x emissions varies substantially among atmospheric chemistry models from -25% to -46% in response to the total NO_x changes from the pre-industrial to present-day period (Thornhill et al., 2021). Because few studies investigated how NO_x from agricultural sources affects CH_4 , it is difficult to assess if the overall impacts of SNO_x -Fer on CH_4 presented in this study based on the GEOS-Chem model are underestimated or

overestimated, even though certain uncertainties are expected. Nevertheless, our results indicate that SNO_x -Fer could be an uncertain but important source in calculating future changes of the global CH_4 budget, the importance of which could increase with future continuing reduction in fossil-fuel NO_x emissions (Rao et al., 2017)

451

452

453

454

455

456457

458

459

460

461

462463

464

465

466

467

468 469

470

471

472

473

474

475

476

477

478 479

480

481

482

483

484

485 486 Beyond the uncertainties remaining in different SNO_x-Fer estimating approaches, an important but also difficult question is how to better evaluate the performances of each method, especially at the regional and global scales. The first-hand meta-data collected from the field experiments is actually not an independent source, as it has been used to establish both of the linear and nonlinear EF methods. More importantly, most of the field experiments are manipulation experiments with artificial fertilizer gradients, which may not fully represent the real-world spatiotemporally varied SNO_x-Fer. Furthermore, we use O₃ data from the national or continental air quality observational networks to evaluate simulated O₃ concentrations as a potential consistency check of the SNO_x-Fer (Fig. S7). However, the uncertainties in SNO_x-Fer are expected to be far less important relative to the uncertainties in the nonlinearity of atmospheric chemistry, emissions of BVOCs or the deposition processes, which together determine the biases between observational and simulated O₃ concentrations. As a result, it is inappropriate to determine the best SNO_x-Fer estimate as the one with the best statistical metrics in O₃ simulation. Moreover, most of the sites that monitor air pollutants are located in the urban regions, where the industrial impacts are far more important than the agricultural sources. A real-time O₃ observational network in the cropland or pasture would be crucial to advance the understandings in SNO_x-Fer and the associated impacts on air quality. Last but not least, the top-down retrievals of NO_x emissions based on satellite NO₂ products could also have the potential to better constrain SNO_x-Fer, while gaps remain in how to precisely isolate the soil NO_x emissions (Bertram et al., 2005; Lin et al., 2024) and even the fertilizer contributions from the total NO_x sources. Synergizing spatiotemporally detailed fertilizer management datasets with the top-down NO_x retrievals with ultra-high resolutions, where the atmospheric NO_x can be assumed to be dominantly affected by the soil sources in agricultural regions, could be one possible solution. However, more work is needed to integrate such big data in the future.

To summarize, with a comprehensive investigation of different approaches to describe SNO_x -Fer, our results reveal the uncertainties in quantifying SNO_x -Fer and the associated important implications in simulating regional air quality and the global greenhouse gas CH_4 . However, the limited number of field experiments impedes accurate assessments of the soil NO_x responses to N fertilizer application as well as improving its representation in both CTMs and TBMs, resulting in large uncertainties in estimates of N fertilizer-induced soil NO_x emissions. We thus highlight the essential necessity to integrate knowledge between agricultural data, atmospheric chemistry modelling and soil biogeochemistry to better represent soil NO_x emissions in models and improve our understanding of the associated effects on air quality and the global CH_4 budget.

487				
488	Acknowledgement			
489	C.G. and S.Z. acknowledge support from the European Commission H2020 programme (Grant-No.			
490	101003536; ESM2025).			
491				
492	Code and data availability			
493	The GEOS-Chem source code can be assessed in https://github.com/geoschem/geos-chem . The CEDS			
494	inventory used in GEOS-Chem can be downloaded at			
495	https://ftp.as.harvard.edu/gcgrid/data/ExtData/HEMCO/CEDS/. The NMIP2 model outputs can be			
496	downloaded through the open-accessed data in Gong et al. (2024).			
497				
498	Author contributions			
499	C.G. designed the study. C.G. performed the GEOS-Chem simulations and data analysis. Y.W. helps			
500	the non-linear EF analysis. H.T. led the NMIP2 projects. S.K, N.V., and S.Z. together contributed to			
501	the simulation of terrestrial biosphere models in NMIP2. C.G. wrote the manuscript. All of the authors			
502	•			
302	contributed to reviewing or editing the manuscript.			
503				
504	Conflict of interest			
505	The authors declare no conflict of interest.			
506				
507	References:			
508	Adalibieke, W., Cui, X. Q., Cai, H. W., You, L. Z., and Zhou, F.: Global crop-specific nitrogen			
509	fertilization dataset in 1961-2020, Scientific Data, 10, 10.1038/s41597-023-02526-z, 2023.			
510	Bates, K. H., Evans, M. J., Henderson, B. H., and Jacob, D. J.: Impacts of updated reaction kinetics on			
511	the global GEOS-Chem simulation of atmospheric chemistry, Geoscientific Model Development, 17,			
512 513	1511-1524, 10.5194/gmd-17-1511-2024, 2024. Bertram, T. H., Heckel, A., Richter, A., Burrows, J. P., and Cohen, R. C.: Satellite measurements of			
514	daily variations in soil NOx emissions -: art. no. L24812, Geophysical Research Letters, 32,			
515	10.1029/2005gl024640, 2005.			
516	Bey, I., Jacob, D. J., Yantosca, R. M., Logan, J. A., Field, B. D., Fiore, A. M., Li, Q. B., Liu, H. G. Y.,			
517	Mickley, L. J., and Schultz, M. G.: Global modeling of tropospheric chemistry with assimilated			
518 519	meteorology: Model description and evaluation, Journal of Geophysical Research-Atmospheres, 106, 23073-23095, 10, 1029/2001id000807, 2001			

- 520 Cheng, W. G., Tsuruta, H., Chen, G. X., and Yagi, K.: N2O and NO production in various Chinese
- agricultural soils by nitrification, Soil Biology & Biochemistry, 36, 953-963,
- 522 10.1016/j.soilbio.2004.02.012, 2004.
- 523 Delmas, R., Serca, D., and Jambert, C.: Global inventory of NOx sources, Nutrient Cycling in
- 524 Agroecosystems, 48, 51-60, 10.1023/a:1009793806086, 1997.
- 525 Du, E. Z. and de Vries, W.: Links Between Nitrogen Limitation and Saturation in Terrestrial
- 526 Ecosystems, Global Change Biology, 31, 10.1111/gcb.70271, 2025.
- East, J. D., Jacob, D. J., Balasus, N., Bloom, A. A., Bruhwiler, L., Chen, Z. C., Kaplan, J. O., Mickley, L. J.,
- Mooring, T. A., Penn, E., Poulter, B., Sulprizio, M. P., Worden, J. R., Yantosca, R. M., and Zhang, Z.:
- 529 Interpreting the Seasonality of Atmospheric Methane, Geophysical Research Letters, 51,
- 530 10.1029/2024gl108494, 2024.
- 531 Eggleston, H., Buendia, L., Miwa, K., Ngara, T., and Tanabe, K.: 2006 IPCC guidelines for national
- 532 greenhouse gas inventories, 2006.
- 533 Erisman, J. W., Galloway, J., Seitzinger, S., Bleeker, A., and Butterbach-Bahl, K.: Reactive nitrogen in
- the environment and its effect on climate change, Current Opinion in Environmental Sustainability,
- 535 3, 281-290, 10.1016/j.cosust.2011.08.012, 2011.
- Fleischer, K., Dolman, A. J., van der Molen, M. K., Rebel, K. T., Erisman, J. W., Wassen, M. J., Pak, B.,
- 537 Lu, X. J., Rammig, A., and Wang, Y. P.: Nitrogen Deposition Maintains a Positive Effect on Terrestrial
- 538 Carbon Sequestration in the 21st Century Despite Growing Phosphorus Limitation at Regional Scales,
- 539 Global Biogeochemical Cycles, 33, 810-824, 10.1029/2018gb005952, 2019.
- 540 Fountoukis, C. and Nenes, A.: ISORROPIA II: a computationally efficient thermodynamic equilibrium
- model for K+-Ca2+-Mg2+-Nh(4)(+)-Na+-SO42--NO3--Cl--H2O aerosols, Atmospheric Chemistry and
- 542 Physics, 7, 4639-4659, 10.5194/acp-7-4639-2007, 2007.
- Fowler, D., Coyle, M., Skiba, U., Sutton, M. A., Cape, J. N., Reis, S., Sheppard, L. J., Jenkins, A.,
- Grizzetti, B., Galloway, J. N., Vitousek, P., Leach, A., Bouwman, A. F., Butterbach-Bahl, K., Dentener,
- 545 F., Stevenson, D., Amann, M., and Voss, M.: The global nitrogen cycle in the twenty-first century,
- Philosophical Transactions of the Royal Society B-Biological Sciences, 368, 10.1098/rstb.2013.0164,
- 547 2013
- 548 Fu, B., Li, J. Y., Jiang, Y. Y., Chen, Z. W., and Li, B. A.: Clean air policy makes methane harder to control
- due to longer lifetime, One Earth, 7, 10.1016/j.oneear.2024.06.010, 2024.
- Goldberg, D. L., Harkey, M., de Foy, B., Judd, L., Johnson, J., Yarwood, G., and Holloway, T.:
- 551 Evaluating NOx emissions and their effect on O3 production in Texas using TROPOMI NO2 and
- 552 HCHO, Atmospheric Chemistry and Physics, 22, 10875-10900, 10.5194/acp-22-10875-2022, 2022.
- 553 Gong, C., Liao, H., Zhang, L., Yue, X., Dang, R. J., and Yang, Y.: Persistent ozone pollution episodes in
- North China exacerbated by regional transport, Environmental Pollution, 265,
- 555 10.1016/j.envpol.2020.115056, 2020.
- Gong, C., Tian, H., Liao, H., Pan, N., Pan, S., Ito, A., Jain, A. K., Kou-Giesbrecht, S., Joos, F., Sun, Q., Shi,
- H., Vuichard, N., Zhu, Q., Peng, C., Maggi, F., Tang, F. H. M., and Zaehle, S.: Global net climate effects
- of anthropogenic reactive nitrogen, Nature, 10.1038/s41586-024-07714-4, 2024.
- Henze, D. K., Hakami, A., and Seinfeld, J. H.: Development of the adjoint of GEOS-Chem, Atmospheric
- 560 Chemistry and Physics, 7, 2413-2433, 10.5194/acp-7-2413-2007, 2007.
- Hergoualc'h, K., Akiyama, H., Bernoux, M., Chirinda, N., Prado, A. d., Kasimir, Å., MacDonald, J. D.,
- Ogle, S. M., Regina, K., and Weerden, T. J. v. d.: N2O emissions from managed soils, and CO2
- 563 emissions from lime and urea application, 2019.
- Hoesly, R. M., Smith, S. J., Feng, L. Y., Klimont, Z., Janssens-Maenhout, G., Pitkanen, T., Seibert, J. J.,
- Vu, L., Andres, R. J., Bolt, R. M., Bond, T. C., Dawidowski, L., Kholod, N., Kurokawa, J., Li, M., Liu, L.,
- Lu, Z. F., Moura, M. C. P., O'Rourke, P. R., and Zhang, Q.: Historical (1750-2014) anthropogenic
- emissions of reactive gases and aerosols from the Community Emissions Data System (CEDS),
- 568 Geoscientific Model Development, 11, 369-408, 10.5194/gmd-11-369-2018, 2018.
- Huber, D. E., Steiner, A. L., and Kort, E. A.: Sensitivity of Modeled Soil NOx Emissions to Soil Moisture,
- Journal of Geophysical Research-Atmospheres, 128, 10.1029/2022jd037611, 2023.

- Hudman, R. C., Moore, N. E., Mebust, A. K., Martin, R. V., Russell, A. R., Valin, L. C., and Cohen, R. C.:
- 572 Steps towards a mechanistic model of global soil nitric oxide emissions: implementation and space
- 573 based-constraints, Atmospheric Chemistry and Physics, 12, 7779-7795, 10.5194/acp-12-7779-2012,
- 574 2012.
- Hurtt, G. C., Chini, L., Sahajpal, R., Frolking, S., Bodirsky, B. L., Calvin, K., Doelman, J. C., Fisk, J.,
- 576 Fujimori, S., Goldewijk, K. K., Hasegawa, T., Havlik, P., Heinimann, A., Humpenoder, F., Jungclaus, J.,
- 577 Kaplan, J. O., Kennedy, J., Krisztin, T., Lawrence, D., Lawrence, P., Ma, L., Mertz, O., Pongratz, J.,
- Popp, A., Poulter, B., Riahi, K., Shevliakova, E., Stehfest, E., Thornton, P., Tubiello, F. N., van Vuuren,
- 579 D. P., and Zhang, X.: Harmonization of global land use change and management for the period 850-
- 580 2100 (LUH2) for CMIP6, Geoscientific Model Development, 13, 5425-5464, 10.5194/gmd-13-5425-
- 581 2020, 2020.
- Janssens-Maenhout, G., Crippa, M., Guizzardi, D., Muntean, M., Schaaf, E., Dentener, F.,
- Bergamaschi, P., Pagliari, V., Olivier, J. G. J., Peters, J., van Aardenne, J. A., Monni, S., Doering, U.,
- Petrescu, A. M. R., Solazzo, E., and Oreggioni, G. D.: EDGAR v4.3.2 Global Atlas of the three major
- greenhouse gas emissions for the period 1970-2012, Earth System Science Data, 11, 959-1002,
- 586 10.5194/essd-11-959-2019, 2019.
- Jiang, Y., Deng, A. X., Bloszies, S., Huang, S., and Zhang, W. J.: Nonlinear response of soil ammonia
- emissions to fertilizer nitrogen, Biology and Fertility of Soils, 53, 269-274, 10.1007/s00374-017-1175-
- 589 3, 2017.
- Jiang, Z., Zhu, R., Miyazaki, K., McDonald, B. C., Klimont, Z., Zheng, B., Boersma, K. F., Zhang, Q.,
- Worden, H., Worden, J. R., Henze, D. K., Jones, D. B. A., van der Gon, H., and Eskes, H.: Decadal
- 592 Variabilities in Tropospheric Nitrogen Oxides Over United States, Europe, and China, Journal of
- 593 Geophysical Research-Atmospheres, 127, 10.1029/2021jd035872, 2022.
- Kou-Giesbrecht, S., Arora, V. K., Seiler, C., Arneth, A., Falk, S., Jain, A. K., Joos, F., Kennedy, D.,
- 595 Knauer, J., Sitch, S., O'Sullivan, M., Pan, N., Sun, Q., Tian, H., Vuichard, N., and Zaehle, S.: Evaluating
- 596 nitrogen cycling in terrestrial biosphere models: a disconnect between the carbon and nitrogen
- 597 cycles, Earth Syst. Dynam., 14, 767-795, 10.5194/esd-14-767-2023, 2023.
- Lin, X. J., Ronald, V., de Laat, J., Huijnen, V., Mijling, B., Ding, J. Y., Eskes, H., Douros, J., Liu, M. Y.,
- 599 Zhang, X., and Liu, Z.: European Soil NOx Emissions Derived From Satellite NO2 Observations, Journal
- of Geophysical Research-Atmospheres, 129, 10.1029/2024jd041492, 2024.
- 601 Liu, S. W., Lin, F., Wu, S., Ji, C., Sun, Y., Jin, Y. G., Li, S. Q., Li, Z. F., and Zou, J. W.: A meta-analysis of
- 602 fertilizer-induced soil NO and combined NO+N₂O emissions, Global Change Biology, 23,
- 603 2520-2532, 10.1111/gcb.13485, 2017.
- 604 Lu, X., Ye, X. P., Zhou, M., Zhao, Y. H., Weng, H. J., Kong, H., Li, K., Gao, M., Zheng, B., Lin, J. T., Zhou,
- 605 F., Zhang, Q., Wu, D. M., Zhang, L., and Zhang, Y. H.: The underappreciated role of agricultural soil
- 606 nitrogen oxide emissions in ozone pollution regulation in North China, Nature Communications, 12,
- 607 10.1038/s41467-021-25147-9, 2021.
- Martin, R. V., Jacob, D. J., Chance, K., Kurosu, T. P., Palmer, P. I., and Evans, M. J.: Global inventory of
- 609 nitrogen oxide emissions constrained by space-based observations of NO₂ columns -:
- art. no. 4537, Journal of Geophysical Research-Atmospheres, 108, 10.1029/2003jd003453, 2003.
- Matson, P. A., Naylor, R., and Ortiz-Monasterio, I.: Integration of environmental, agronomic, and
- economic aspects of fertilizer management, Science, 280, 112-115, 10.1126/science.280.5360.112,
- 613 1998
- 614 Nicholas Hutchings, J. Webb, and Amon, B.: EMEP/EEA air pollutant emission inventory guidebook
- 615 2023: 3.D Agricultural soils 2023, 2023.
- 616 Park, R. J., Jacob, D. J., Field, B. D., Yantosca, R. M., and Chin, M.: Natural and transboundary
- 617 pollution influences on sulfate-nitrate-ammonium aerosols in the United States: Implications for
- 618 policy, Journal of Geophysical Research-Atmospheres, 109, 10.1029/2003jd004473, 2004.
- 619 Peng, S. S., Lin, X., Thompson, R. L., Xi, Y., Liu, G., Hauglustaine, D., Lan, X., Poulter, B., Ramonet, M.,
- 620 Saunois, M., Yin, Y., Zhang, Z., Zheng, B., and Ciais, P.: Wetland emission and atmospheric sink
- changes explain methane growth in 2020, Nature, 612, 477-+, 10.1038/s41586-022-05447-w, 2022.

- 622 Pinder, R. W., Davidson, E. A., Goodale, C. L., Greaver, T. L., Herrick, J. D., and Liu, L. L.: Climate
- change impacts of US reactive nitrogen, Proceedings of the National Academy of Sciences of the
- 624 United States of America, 109, 7671-7675, 10.1073/pnas.1114243109, 2012.
- Rao, S., Klimont, Z., Smith, S. J., Van Dingenen, R., Dentener, F., Bouwman, L., Riahi, K., Amann, M.,
- 626 Bodirsky, B. L., van Vuuren, D. P., Reis, L. A., Calvin, K., Drouet, L., Fricko, O., Fujimori, S., Gernaat, D.,
- Havlik, P., Harmsen, M., Hasegawa, T., Heyes, C., Hilaire, J., Luderer, G., Masui, T., Stehfest, E.,
- 628 Strefler, J., van der Sluis, S., and Tavoni, M.: Future air pollution in the Shared Socio-economic
- Pathways, Global Environmental Change-Human and Policy Dimensions, 42, 346-358,
- 630 10.1016/j.gloenvcha.2016.05.012, 2017.
- Rubin, H. J., Fu, J. S., Dentener, F., Li, R., Huang, K., and Fu, H. B.: Global nitrogen and sulfur
- deposition mapping using a measurement-model fusion approach, Atmospheric Chemistry and
- 633 Physics, 23, 7091-7102, 10.5194/acp-23-7091-2023, 2023.
- Russell, A. R., Perring, A. E., Valin, L. C., Bucsela, E. J., Browne, E. C., Min, K. E., Wooldridge, P. J., and
- 635 Cohen, R. C.: A high spatial resolution retrieval of NO₂ column densities from OMI:
- method and evaluation, Atmospheric Chemistry and Physics, 11, 8543-8554, 10.5194/acp-11-8543-
- 637 2011, 2011.
- 638 Shcherbak, I., Millar, N., and Robertson, G. P.: Global metaanalysis of the nonlinear response of soil
- 639 nitrous oxide (N2O) emissions to fertilizer nitrogen, Proceedings of the National Academy of
- Sciences of the United States of America, 111, 9199-9204, 10.1073/pnas.1322434111, 2014.
- 641 Skiba, U., Medinets, S., Cardenas, L. M., Carnell, E. J., Hutchings, N., and Amon, B.: Assessing the
- contribution of soil NO<i><sub></i>>< emissions to European atmospheric pollution,
- 643 Environmental Research Letters, 16, 10.1088/1748-9326/abd2f2, 2021.
- Stehfest, E. and Bouwman, L.: N2O and NO emission from agricultural fields and soils under natural
- vegetation:: summarizing available measurement data and modeling of global annual emissions,
- 646 Nutrient Cycling in Agroecosystems, 74, 207-228, 10.1007/s10705-006-9000-7, 2006.
- 647 Steinkamp, J. and Lawrence, M. G.: Improvement and evaluation of simulated global biogenic soil NO
- emissions in an AC-GCM, Atmospheric Chemistry and Physics, 11, 6063-6082, 10.5194/acp-11-6063-
- 649 2011, 2011.
- Thornhill, G. D., Collins, W. J., Kramer, R. J., Olivi, D., Skeie, R. B., O'Connor, F. M., Abraham, N. L.,
- 651 Checa-Garcia, R., Bauer, S. E., Deushi, M., Emmons, L. K., Forster, P. M., Horowitz, L. W., Johnson, B.,
- Keeble, J., Lamarque, J. F., Michou, M., Mills, M. J., Mulcahy, J. P., Myhre, G., Nabat, P., Naik, V.,
- Oshima, N., Schulz, M., Smith, C. J., Takemura, T., Tilmes, S., Wu, T. W., Zeng, G., and Zhang, J.:
- 654 Effective radiative forcing from emissions of reactive gases and aerosols a multi-model comparison,
- 655 Atmospheric Chemistry and Physics, 21, 853-874, 10.5194/acp-21-853-2021, 2021.
- 656 Tian, H., Pan, N., Thompson, R. L., Canadell, J. G., Suntharalingam, P., Regnier, P., Davidson, E. A.,
- 657 Prather, M., Ciais, P., Muntean, M., Pan, S., Winiwarter, W., Zaehle, S., Zhou, F., Jackson, R. B.,
- Bange, H. W., Berthet, S., Bian, Z., Bianchi, D., Bouwman, A. F., Buitenhuis, E. T., Dutton, G., Hu, M.,
- 659 Ito, A., Jain, A. K., Jeltsch-Thömmes, A., Joos, F., Kou-Giesbrecht, S., Krummel, P. B., Lan, X., Landolfi,
- A., Lauerwald, R., Li, Y., Lu, C., Maavara, T., Manizza, M., Millet, D. B., Mühle, J., Patra, P. K., Peters,
- 661 G. P., Qin, X., Raymond, P., Resplandy, L., Rosentreter, J. A., Shi, H., Sun, Q., Tonina, D., Tubiello, F.
- N., van der Werf, G. R., Vuichard, N., Wang, J., Wells, K. C., Western, L. M., Wilson, C., Yang, J., Yao,
- 663 Y., You, Y., and Zhu, Q.: Global nitrous oxide budget (1980–2020), Earth Syst. Sci. Data, 16, 2543-
- 664 2604, 10.5194/essd-16-2543-2024, 2024.
- Tian, H. Q., Bian, Z. H., Shi, H., Qin, X. Y., Pan, N. Q., Lu, C. Q., Pan, S. F., Tubiello, F. N., Chang, J. F.,
- 666 Conchedda, G., Liu, J. G., Mueller, N., Nishina, K., Xu, R. T., Yang, J., You, L. Z., and Zhang, B. W.:
- History of anthropogenic Nitrogen inputs (HaNi) to the terrestrial biosphere: a 5 arcmin resolution
- annual dataset from 1860 to 2019, Earth System Science Data, 14, 4551-4568, 10.5194/essd-14-
- 669 4551-2022, 2022.
- 670 Tian, H. Q., Yang, J., Xu, R. T., Lu, C. Q., Canadell, J. G., Davidson, E. A., Jackson, R. B., Arneth, A.,
- 671 Chang, J. F., Ciais, P., Gerber, S., Ito, A., Joos, F., Lienert, S., Messina, P., Olin, S., Pan, S. F., Peng, C.
- H., Saikawa, E., Thompson, R. L., Vuichard, N., Winiwarter, W., Zaehle, S., and Zhang, B. W.: Global

- soil nitrous oxide emissions since the preindustrial era estimated by an ensemble of terrestrial
- 674 biosphere models: Magnitude, attribution, and uncertainty, Global Change Biology, 25, 640-659,
- 675 10.1111/gcb.14514, 2019.
- Wang, Y., Yao, Z. S., Zheng, X. H., Subramaniam, L., and Butterbach-Bahl, K.: A synthesis of nitric
- 677 oxide emissions across global fertilized croplands from crop-specific emission factors, Global Change
- 678 Biology, 28, 4395-4408, 10.1111/gcb.16193, 2022.
- Wang, Y., Ge, C., Garcia, L. C., Jenerette, G. D., Oikawa, P. Y., and Wang, J.: Improved modelling of
- soil NOx emissions in a high temperature agricultural region: role of background emissions on NO2
- trend over the US, Environmental Research Letters, 16, 10.1088/1748-9326/ac16a3, 2021.
- Wang, Y., Yao, Z. S., Pan, Z. L., Guo, H. J., Chen, Y. C., Cai, Y. J., and Zheng, X. H.: Nonlinear response
- of soil nitric oxide emissions to fertilizer nitrogen across croplands, Biology and Fertility of Soils, 60,
- 684 483-492, 10.1007/s00374-024-01818-9, 2024.
- 685 Weng, H. J., Lin, J. T., Martin, R., Millet, D. B., Jaegle, L., Ridley, D., Keller, C., Li, C., Du, M. X., and
- Meng, J.: Global high-resolution emissions of soil NOx, sea salt aerosols, and biogenic volatile organic
- 687 compounds, Scientific Data, 7, 10.1038/s41597-020-0488-5, 2020.
- Yienger, J. J. and Levy, H.: EMPIRICAL-MODEL OF GLOBAL SOIL-BIOGENIC NOX EMISSIONS, Journal of
- 689 Geophysical Research-Atmospheres, 100, 11447-11464, 10.1029/95jd00370, 1995.
- 690 Yuan, H., Dai, Y. J., Xiao, Z. Q., Ji, D. Y., and Shangguan, W.: Reprocessing the MODIS Leaf Area Index
- 691 products for land surface and climate modelling, Remote Sensing of Environment, 115, 1171-1187,
- 692 10.1016/j.rse.2011.01.001, 2011.
- 693 Zaehle, S. and Dalmonech, D.: Carbon-nitrogen interactions on land at global scales: current
- 694 understanding in modelling climate biosphere feedbacks, Current Opinion in Environmental
- 695 Sustainability, 3, 311-320, 10.1016/j.cosust.2011.08.008, 2011.
- Zaehle, S. and Friend, A. D.: Carbon and nitrogen cycle dynamics in the O-CN land surface model: 1.
- 697 Model description, site-scale evaluation, and sensitivity to parameter estimates, Global
- 698 Biogeochemical Cycles, 24, 10.1029/2009gb003521, 2010.
- 699 Zhai, S. X., Jacob, D. J., Wang, X., Liu, Z. R., Wen, T. X., Shah, V., Li, K., Moch, J. M., Bates, K. H., Song,
- 700 S. J., Shen, L., Zhang, Y. Z., Luo, G., Yu, F. Q., Sun, Y. L., Wang, L. T., Qi, M. Y., Tao, J., Gui, K., Xu, H. H.,
- 701 Zhang, Q., Zhao, T. L., Wang, Y. S., Lee, H. C., Choi, H., and Liao, H.: Control of particulate nitrate air
- 702 pollution in China, Nature Geoscience, 14, 389-+, 10.1038/s41561-021-00726-z, 2021.
- 703 Zhang, R. Y., Tie, X. X., and Bond, D. W.: Impacts of anthropogenic and natural NO_x
- sources over the US on tropospheric chemistry, Proceedings of the National Academy of Sciences of
- 705 the United States of America, 100, 1505-1509, 10.1073/pnas.252763799, 2003.
- 706 Zhao, Y., Saunois, M., Bousquet, P., Lin, X., Hegglin, M. I., Canadell, J. G., Jackson, R. B., and Zheng, B.:
- 707 Reconciling the bottom-up and top-down estimates of the methane chemical sink using multiple
- 708 observations, Atmos. Chem. Phys., 23, 789-807, 10.5194/acp-23-789-2023, 2023.
- 709 Zhao, Y. H., Zheng, B., Saunois, M., Ciais, P., Hegglin, M. I., Lu, S. M., Li, Y. F., and Bousquet, P.: Air
- 710 pollution modulates trends and variability of the global methane budget, Nature, 642,
- 711 10.1038/s41586-025-09004-z, 2025.